



## Performance of CDF for $B$ physics

R.G.C. Oldeman  
for the CDF collaboration

University of Pennsylvania, Philadelphia

Hadron colliders can be an abundant source of heavy flavor, but pose a challenge to isolate the physics signals from the high backgrounds. The upgraded CDF II detector, with its precise tracking capabilities and powerful trigger system, is well equipped for this task. The detector is described with an emphasis on actual performance and on techniques to maximize the heavy flavor yield. Some first heavy flavor results are summarized.

### 1 Introduction

In Run I of the Tevatron, CDF made essential contributions to  $B$  physics, providing some of the best measurements of masses, lifetimes, mixing and branching ratios. The  $B$  factories are now setting new standards with a wealth of precision measurements, posing stringent tests of the standard model. CDF has made significant improvements of the detector and the trigger to expand its capabilities beyond simply profiting from the higher luminosities of the Tevatron in Run II.

Both  $B$  and  $D$  mesons are amply produced at the Tevatron: in Run I the  $B^+$  cross section with transverse momentum  $p_T \geq 6 \text{ GeV}/c$  and rapidity  $|y| \leq 1$  was measured in the  $B^+ \rightarrow J/\psi K^+$  mode to be  $3.6 \pm 0.6 \mu\text{b}$  [1]. A new preliminary Run II measurement of the charm meson cross sections for the same kinematic region yields even larger values:  $4.3 \pm 0.7 \mu\text{b}$  for  $D^+$  and  $9.3 \pm 1.1 \mu\text{b}$  for  $D^0$ , both measured using fully reconstructed hadronic decays.

Heavy flavor cross sections at hadron colliders are three orders of magnitude larger than at  $e^+e^-$  machines running at the  $\Upsilon(4S)$ , and include the heavier  $B_s$  and  $B_c$  mesons and the weakly decaying baryons  $\Lambda_b$  and  $\Xi_b$ . The challenge at a hadron collider is to select in real time the heavy flavor events from the overwhelming QCD background. Therefore the emphasis in this talk is on the trigger system, which is a particular strength of CDF II.

### 2 Performance of the Tevatron

The center-of-mass energy of the Tevatron has increased from 1.8 TeV in Run I to 1.96 TeV in Run II, and the number of proton and anti-proton bunches has increased from 6 to 36, with a bunch separation of 396 ns. We anticipate the number of interactions per bunch crossing to rise from 1.2 at present peak luminosities of  $4 \times 10^{31} \text{ cm}^{-2}\text{s}^{-1}$  to 6 at future luminosities

of  $2 \times 10^{32} \text{ cm}^{-2}\text{s}^{-1}$ . This number can be reduced by increasing the number of bunches, but the upgrade to 132 ns bunch spacing has been indefinitely postponed. At the time of this workshop, the Tevatron has delivered  $190 \text{ pb}^{-1}$ , of which CDF has recorded  $145 \text{ pb}^{-1}$  on tape. Present  $B$  physics analyses use up to  $70 \text{ pb}^{-1}$  of this data, where the selection criterion with the largest rejection came from requiring stable operation of the silicon detector.

### 3 The CDF II detector

CDF II [2] has the typical structure of a  $4\pi$  detector at a symmetric collision point. A superconducting solenoid provides a uniform 1.4 T field over a tracking volume of  $34 \text{ m}^3$ . Closest to the beam is a silicon system to provide an accurate measurement of the impact parameter of charged tracks. A large-radius, low-material drift chamber gives accurate measurements of tens of charged particles per interaction. New in Run II is a Time-of-Flight (TOF) detector for particle identification at low momenta. Outside the magnet are calorimeter systems followed by muon identification systems. The components most relevant for  $B$  physics are described in more detail below.

#### 3.1 The Silicon system

CDF II has three silicon systems [3]. Layer 00 (L00) is a single-sided low-mass radiation-hard silicon detector, mounted on the beryllium beam pipe at a radius of 1.6 cm. The SVX II is a five-layer double-sided silicon strip detector. It consists of 3 barrels, each 30 cm in length and covers 90% of the extended interaction region ( $\text{RMS} \approx 30 \text{ cm}$ ). The Intermediate Silicon Layer (ISL) provides one additional double-sided layer in the central region and two in the forward and backward regions, to improve track reconstruction using silicon only. A light-weight carbon-fiber space frame keeps the  $3.5 \text{ m}^2$  of ISL sensors stably aligned at the  $10 \mu\text{m}$

level. All silicon sensors use the same 128 channel SVXIII readout chip that uses an analog pipeline for deadtimeless operation. The silicon system has  $\approx 750k$  channels in total and can be readout in  $20 \mu s$ .

### 3.2 Commissioning the silicon detector

In the first year of data-taking, CDF has faced many startup problems with the silicon system that have now mostly been overcome. The SVXII has suffered from several beam incidents where a relatively small amount of radiation was incident on the silicon sensors and chips within a few nanoseconds, resulting in the permanent loss of several sensors. The Tevatron has now installed interlocks to prevent this class of beam incidents. Other damage occurred when the silicon detector was read out at fixed frequencies of several kHz during anomalous trigger conditions. This has been traced down to resonant oscillations of wirebonds perpendicular to the 1.4 T magnetic field. CDF has now implemented hardware protection against fixed-frequency readout. The ISL suffered from insufficient cooling as 11 of the 12 cooling lines were internally blocked with epoxy at some  $90^\circ$  elbow connections. Using boroscopes to find the blockages and a pulsed 40 W laser to destroy them, 10 of the 11 blocked lines have now been cleared. L00 is affected by pickup from the digital readout lines on the analog signal cables. Methods have been developed to correct for this in software, but they require non-sparsified readout, prohibiting the use of L00 in the trigger. The CAEN power supplies that supply the L00 sensors with the bias voltage suffered from beam related failures. This has been solved by replacing the MOSFET voltage regulator by a BJT circuit. At the time of this workshop more than 90% of the silicon detector is operational and used in physics analyses. One disadvantage of the present silicon detector is the large amount of passive material inside the tracking region: a track traverses on average  $\approx 15\%$  of a radiation length.

### 3.3 The Central Outer Tracker (COT)

The Central Outer Tracker [4] is a cylindrical Ar/Et drift chamber based on the highly successful CTC used in Run I, modified to cope with the shorter time between interactions. The COT has 96 layers, organized in 8 super layers, alternating between axial and  $\pm 2^\circ$  stereo readout. The single-wire resolution is  $\approx 200 \mu m$ , resulting in a momentum resolution of  $\frac{\Delta p_T}{p_T} \approx (0.7 \pm 0.1 p_T)\%$ . The measurement of the specific energy deposition  $dE/dx$  gives a  $\pi/K$  separation of  $\approx 1.2\sigma$  in the region of the relativistic rise ( $p_T \geq 2 \text{ GeV}$ ). The COT has proven to be a very reliable detector, with fewer than 1% dead channels. The tracking efficiency for high- $p_T$  isolated tracks has been

measured from data using  $W^+ \rightarrow e^+ \nu_e$  events to be better than 99.5%.

### 3.4 The Time-of-Flight detector

For the first time at a hadron collider experiment, CDF II has installed a Time of Flight (TOF) detector for particle identification. It consists of 216 scintillator bars, 3 m long and  $4 \times 4 \text{ cm}$  in cross section, mounted between the COT and the superconducting solenoid. The bars are read out on both sides by compact fine-mesh 19-stage photomultipliers, that allow operation inside the full 1.4 T magnetic field. The achieved timing resolution is 120 ps, close to the 100 ps design, giving  $2\sigma$  separation between pions and kaons up to momenta of  $1.5 \text{ GeV}/c$ . The TOF has been designed primarily to improve  $B$  flavor tagging, in particular for the  $B_s$ , which is often produced together with a kaon, correlated in charge to the  $b$  quark produced. The TOF has also found use for proton identification, cosmic ray rejection and monopole searches. The TOF performs reliably and all 432 channels are fully functional. However, the occupancy of  $\approx 20\%$  is about two times higher than expected, which has affected the reconstruction efficiency.

## 4 The three-level trigger

CDF uses a three-level trigger system to reduce the 1.7 MHz bunch crossing rate to 75 Hz written on tape. The first trigger level is deadtimeless, with a 42 buffer deep pipelined system, allowing  $5 \mu s$  to form a trigger decision. The eXtremely Fast Tracker (XFT) [5] reconstructs COT tracks in the axial projection down to transverse momenta of  $1.5 \text{ GeV}/c$ , using hits with coarse timing information. Muon and electron signals can also be matched to tracks. Information about energy deposition in the hadron calorimeter are available at Level 1, but are not used for  $B$  triggers. The maximum input rate for Level 2 is presently about 20 kHz. We expect this to reach 25 kHz soon, but the original design rate of 50 kHz will be difficult to reach. At Level 2, the Silicon Vertex Tracker (SVT) [6] provides a list of tracks using axial hits of 4 silicon layers. This allows to select displaced tracks, which greatly enhances the purity of heavy flavor signals. Typical rate reductions are  $O(10^{-1})$  when requiring one track with a displacement of  $\geq 100 \mu m$ , or  $O(10^{-2})$  when requiring two displaced tracks. Further trigger rate reductions are achieved when selecting on the opening angle between two tracks, requiring positive lifetime or pointing of the two-track momentum vector to the primary vertex. The readout time of the COT currently limits the rate into the third trigger level to  $\leq 250 \text{ Hz}$ . At Level 3, the complete events are processed on a farm of 300 PCs, which perform full event

reconstruction and write up to 20 MB/s to tape. The event size of almost 300 kB limits the Level3 output rate to  $\leq 75$  Hz, but data compression techniques are being developed to increase this to more than 100 Hz.

## 5 Trigger strategies

The vast majority of  $B$  physics at CDF is based on three sets of triggers. The *dimuon* trigger requires two muons with  $p_T \geq 1.5$  GeV/c. It collects vast samples of  $J/\psi \rightarrow \mu^+ \mu^-$  decays, which are  $\approx 15\%$  from  $B$  decay. At present peak luminosities this trigger uses 40 Hz at Level2 and new hardware is being built to select on the transverse mass of a muon pair, which should reduce this rate significantly. The *lepton+displaced track* trigger uses muons and electrons with  $p_T \geq 4$  GeV/c combined with a displaced track found by the SVT. The specific yield of semileptonic  $B$  decays with this trigger is 5 times higher than in the Run I equivalent, which was based on an 8 GeV/c lepton. These signals are used for lifetime measurements and for optimizing flavor tagging algorithms. The *two-track* trigger requires two displaced tracks. One version requires a large opening angle and pointing to the primary vertex. It is designed to collect 2-body  $B$  decays, such as  $B_d \rightarrow \pi^+ \pi^-$ . The other requires smaller opening angles and has stricter requirements on the track displacement (120  $\mu\text{m}$  instead of 100  $\mu\text{m}$ ). This second version is designed for multi-body  $B$  decays, such as  $B_s \rightarrow D_s^- \pi^+$ ; it has also proven useful for collecting huge samples of hadronic  $D$  meson decays. The two-track trigger uses almost all of the available Level1 bandwidth and a significant fraction of the bandwidth at Level3. We are constantly trying to reduce the trigger rates while keeping the maximum amount of real heavy flavor.

## 6 Techniques for optimizing heavy flavor yields

### 6.1 Dynamic prescaling

A typical “store” at the Tevatron lasts about 20 hours, during which time the luminosity has decreased by a factor 2.5 with respect to the initial luminosity. Since the trigger bandwidth has been designed for peak luminosity, significant bandwidth is available in the later part of a store. We have developed techniques to fill this available bandwidth with  $B$  physics by implementing triggers with several different  $p_T$  thresholds and increasing the acceptance fraction (prescale) of the triggers with lower thresholds as the luminosity decreases. The two-track trigger comes in three versions. The *high- $p_T$*  trigger has a low rate due to high thresholds (two oppositely charged tracks of

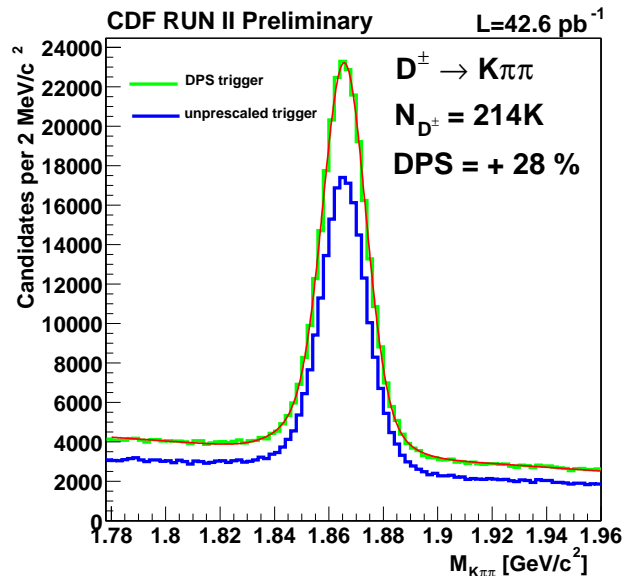


**Figure 1.** Event yield of  $D^+ \rightarrow K^+ \pi^- \pi^-$  since the introduction of dynamic prescaling. Blue curve is the  $D^+$  yield of the nominal trigger, the green curve is the  $D^+$  total yield including the low- $p_T$  trigger that was effectively prescaled by a factor 0.22. outside

$p_T \geq 2.5$  GeV/c with  $\Sigma p_T \geq 6.5$  GeV/c) and is never prescaled. The rate is low enough that it can be safely run up to luminosities of  $8 \times 10^{31} \text{ cm}^{-2} \text{ s}^{-1}$ . The *nominal* trigger requires two oppositely charged tracks of  $p_T \geq 2.0$  GeV/c with  $\Sigma p_T \geq 5.5$  GeV/c. This trigger is prescaled when the Level1 accept rate exceeds 20 kHz. A *low- $p_T$*  trigger that requires two tracks of  $p_T \geq 2.0$  GeV/c and no  $\Sigma p_T$  or opposite charge requirement is enabled when the Level1 accept rate drops below 16 kHz. In the six months that dynamic prescaling has been enabled, the low- $p_T$  trigger has given a yield increase of 28% in the  $D^+ \rightarrow K^+ \pi^- \pi^-$  channel, as shown in Figure 1, while it was prescaled on average by a factor 4.5.

### 6.2 XFT 1-miss configuration

Until October 2002, the XFT required 10 out of 12 hits on the four axial superlayers of the COT to reconstruct a track. This resulted in an efficiency of  $>95\%$ , but with a purity that was considered insufficient. Studies showed that the COT single hit efficiency was high enough that requiring 11 out of 12 hits resulted in an efficiency still better than 90%, while reducing the rate of the two-track trigger by almost a factor two at high luminosity.

SVT efficiency

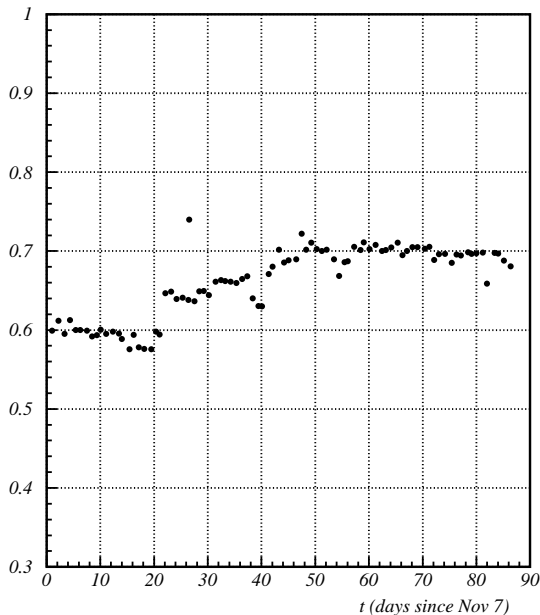


**Figure 2.** Efficiency of the SVT in days since Nov 7, 2002. The rise in efficiency from 60% to 70% comes from improved SVX coverage. The high point at  $t = 26$  corresponds to a test run with 4/5 SVT tracking.

### 6.3 4/5 SVT tracking

The Silicon Vertex Tracker requires the presence of four strip clusters in four layers, resulting in an overall efficiency that scales as the fourth power of the single hit efficiency. It is possible to program the SVT to use all five SVX layers, and allow a missing hit in one layer. In a test-run, we found a 15% increase of the SVT single-track efficiency, as shown in Figure 2. This will result in a significant increase of the heavy flavor yields from the two-track trigger. However, the trigger rate at Level 2 rises by 70% and we are studying how to improve the purity.

### 6.4 Silicon tracking at Level 3

While the core of the impact parameter resolution of the SVT is similar to the offline resolution (both  $\approx 50 \mu\text{m}$ , including a contribution of  $\approx 35 \mu\text{m}$  from the beamspot), the SVT impact parameter measurement has significant non-Gaussian tails, which can be attributed to the handling of large clusters of overlapping hits in the silicon detector. The reconstruction software at Level 3 can reduce the non-Gaussian resolution tails because more time and more information are available for complex pattern recognition and the handling of overlapping hits. In May 2003, silicon tracking at Level 3 was implemented and resulted in a factor 2 reduction of the rate to tape of the two-

track trigger with a small ( $\approx 5\%$ ) loss of heavy flavor signal.

## 7 Some recent results

The low  $p_T$  threshold of the dimuon trigger has made it possible to collect  $J/\psi$  decays down to zero transverse momentum. We measured a cross section  $\sigma(J/\psi)_{|y| \leq 0.6} \times B(J/\psi \rightarrow \mu\mu) = 240 \pm 1(\text{stat})_{-28}^{+35}(\text{syst}) \text{ nb}$ . Using fully reconstructed  $B \rightarrow J/\psi X$  decays we measure:  $\tau(B^+) = 1.57 \pm 0.07(\text{stat}) \pm 0.02(\text{syst}) \text{ ps}$ ,  $\tau(B^0) = 1.42 \pm 0.09(\text{stat}) \pm 0.02(\text{syst}) \text{ ps}$ , and  $\tau(B_s) = 1.25 \pm 0.20(\text{stat}) \pm 0.02(\text{syst}) \text{ ps}$ .

In the two-track trigger, we have reconstructed 450k  $D^0 \rightarrow K^- \pi^+$  decays. We looked for  $D^0 \rightarrow \mu^+ \mu^-$  decays, found zero events on a background of 1.7, and set a preliminary limit of  $2.7 \times 10^{-6}$  at 90% CL. We also looked for direct CP violation in  $D^*$ -tagged  $D^0 \rightarrow \pi^+ \pi^-$  and  $D^0 \rightarrow K^+ K^-$  decays and find  $A_{CP, KK} = 2.0 \pm 1.7(\text{stat}) \pm 0.6(\text{syst})\%$  and  $A_{CP, \pi\pi} = 3.0 \pm 1.9(\text{stat}) \pm 0.6(\text{syst})\%$ .

## References

1. D. Acosta *et al.* [CDF Collaboration], Phys. Rev. D **65**, 052005 (2002).
2. R. Blair *et al.* [CDF-II Collaboration], FERMILAB-PUB-96-390-E.
3. A. Sill [CDF Collaboration], Nucl. Instrum. Meth. A **447**, 1 (2000).
4. K. T. Pitts [CDF Collaboration], Nucl. Phys. Proc. Suppl. **61B**, 230 (1998).
5. E. J. Thomson *et al.*, IEEE Trans. Nucl. Sci. **49**, 1063 (2002).
6. W. Ashmanskas *et al.* [CDF Collaboration], Nucl. Instrum. Meth. A **447**, 218 (2000).